Am J Transl Res 2021;13(4):3806-3810
www.ajtr.org /ISSN:1943-8141/AJTR0125888

*Original Article*

# Application and comparative analysis of 3.0T MRI and ultrasound in diagnosing CSP after caesarean section

Dongxue Yang[1*], Zhao Zhang[2*], Zhilei Kang[2], Yajing Liu[2]

*[1]Department of Ultrasound, The People's Hospital of Hengshui City, Hengshui 053000, China; [2]Image Center, The People's Hospital of Hengshui City, Hengshui 053000, China. [*]Equal contributors and co-first authors.*

Received November 8, 2020; Accepted December 21, 2020; Epub April 15, 2021; Published April 30, 2021

**Abstract:** Objective: To investigate the effect of 3.0T MRI and ultrasonography in the diagnosis of uterine scar pregnancy (CSP) after caesarean section, and to compare their diagnostic value for CSP. Materials and Methods: A retrospective analysis was conducted on 60 patients with CSP treated in our hospital over a period of July 2018 to March 2020. All patients underwent 3.0T MRI, ultrasonography, and surgical termination of pregnancy and pathological analysis. The value of 3.0T MRI and ultrasonography in the diagnosis of CSP was analyzed. Results: (1) The 60 patients were pathologically analyzed. Among these patients, 2 of whom were trophoblastic diseases, 5 were pregnancy abortion, 8 were cervical pregnancy, and 45 were CSP. (2) The results of ultrasound detection were 37 cases of CSP, 7 cases of misdiagnosis, and 8 cases of missed diagnosis; 3.0T MRI results were 44 cases of CSP, 1 case of misdiagnosis, and 1 case of missed diagnosis. (3) The sensitivity (97.78%), specificity (93.33%), coincidence rate (96.67%), positive diagnosis rate (97.78%), negative diagnosis rate (93.33%), AUC (0.973), and 95% CI (0.914-0.996) of 3.0T MRI in diagnosing CSP were significantly higher than those of ultrasound diagnosis (82.22%, 53.33%, 84.09%, 84.09%, 50%, 0.681, 0.051-0.776) (P<0.05). Conclusion: The coincidence rate of 3.0T MRI in the diagnosis of CSP after caesarean section is significantly better than that of ultrasound diagnosis, and it can be used to provide reference for clinical diagnosis of CSP after cesarean section.

**Keywords:** 3.0T MRI, ultrasound, planned uterine delivery, postoperative, uterine scar pregnancy, application effect

## Introduction

Nowadays, the cesarean section rate in China is mounting on a yearly basis, and it can reach nearly 54.74% [1-3]. Due to the fissure after cesarean section of the lower uterus and the fact that pregnant egg was implanted and planted at the incision of the endometrial defect, the cesarean scar pregnancy (CSP) is easy to occur. As the rate of cesarean section rises, the incidence of CSP after cesarean delivery is also on the rise [4]. Since there are more fibrous tissues and thin muscle walls in the uterine scar, pregnancy can cause complications such as hemorrhage and uterine rupture, which seriously threat the patient's life and safety. For this reason, early diagnosis and treatment are extremely critical for improving CSP after uterine delivery. Because CSP has no specific clinical manifestations, misdiagnosis and missed diagnosis are commonly seen. Once it is misdiagnosed as an early intrauterine pregnancy, the use of drugs or artificial abortion will cause major bleeding [5-7]. Ultrasound detection is simple, straightforward and non-invasive in clinical practice, and it is common to diagnose CSP today. However, ultrasound detection sometimes fails to locate the implantation site of the gestational sac, and cannot accurately determine the depth of the implantation of the gestational sac into the muscle layer. MRI has the characteristics of multi-directional, multi-layer and multi-parameter imaging. With the good resolution, it can clearly show the relationship between cesarean section scars and gestational sac [8].

This research innovatively uses 3.0T MRI, which has more stable magnets to ensure the normal operation of MRI; the application of dual gradients of dynamic speed increase improves the signal-to-noise ratio and eliminates artifacts

caused by phase errors, and the layer thickness is thinner, and the resolution is higher. The dual-source four-point elliptical radio frequency field overcomes the uneven radio frequency field caused by the human body entering the magnetic field. On the other hand, the "dual-source four-point excitation" forms an ellipsoidal radio frequency field in the magnet to achieve a physiological curve with the human body. The uniform radio frequency excitation volume eliminates the dielectric artifacts that appear in a large range of scanning due to the shorter wavelength caused by the increase of the 3.0T frequency, so as to truly obtain excellent image quality. This study explored the application of 3.0T magnetic resonance imaging (MRI) and ultrasound in diagnosing CSP and comparatively analyzed their diagnostic value for CSP, aiming to provide a favorable reference for the clinical diagnosis and treatment of CSP.

## Materials and methods

### *General information*

We retrospectively analyzed the clinical data of 60 patients with CSP who were admitted to our hospital from July 2018 to March 2020. All patients underwent 3.0T MRI, ultrasound examination, surgical termination of pregnancy, and pathological analysis. Patients aged 23-42 years old, and the average age was (32.56±5.08) years; menopause time was 41 d-105 d, and the average was (54.28±11.05) days; the interval from the previous cesarean section was 9 months to 16 years, with an average of (4.25±2.38) years; 53 patients had irregular vaginal bleeding, 42 of them had mild abdominal pain, and 16 had no apparent clinical symptoms. This study has been approved by the hospital ethics committee and written consent forms were obtained from patients and their families.

### *Ultrasonic inspection*

The pregnant woman was in the lithotomy position for transvaginal examination, and the Accuson Sequoia 512 Doppler ultrasonic diagnostic apparatus (Siemens) was selected for detection. The probe frequency was set to 5 MHz-7.5 MHz, and the gestational sac shape, size and blood flow signal and echo of the gestational sac were measured. And the presence or absence of fetal heart beats and germs were observed. The relationship between the CSP in the lower uterus and the gestational sac was detected, and the thickness of the scar in the lower uterus was measured.

### *3.0T MRI inspection*

Prior inspection, the patient was informed of the precautions and the breath-hold training was performed. The 3.0T verio MRI was selected for the inspection. Among them, there are 8 patients with pelvic plain scan and 52 patients with pelvic plain scan combined with enhanced detection. A 16-channel phased array body surface coil was used to scan the patient's pelvic cavity with coronal, sagittal and axial T1 and T2 weighted imaging using fast spin echo sequence. Enhanced scan: Gadolinium (Gd-DTPA) contrast agent was injected through the elbow vein, with the contrast agent flow rate of 2.0 Ml/s. And the VIBE volumetric interpolation method was used to scan the sagittal and axial positions with the breath-hold sequence, and the coronal position was added in some patients. Scan parameters: T1W1: TE11ms, TR836ms, F0V320×285, 140° is the flip angle, 5 mm is the layer thickness; T2W1: TE108ms, TR4000ms, F0V320×100, 150° is the flip angle, 5 mm is the layer thickness; VIBE detection: TE1.44ms, tr4.08ms, F0V320×100, 9° is the flip angle, 5 mm is the layer thickness, using the breath-hold fast scanning method.

Two associate chief physicians of our hospital jointly performed the image reading and analysis. The gestational sac shape, size and the positional relationship of the surgical scar, the position of the scar on the surgical incision were observed; the myometrium and gestational sac were analyzed; the organ situation surrounding uterus was checked. When there was not much consensus, the two associate chief physicians discuss and negotiate together to reach the final result.

### *Statistical analysis*

All analyses were conducted using IBM SPSS Statistics 19.0. The count data was represented by [n (%)], and the $X^2$ test was used for the comparison. $P<0.05$ indicated that the difference was statistically significant.

**Table 1.** Pathological diagnosis results

| Pathological diagnosis results | Number | Constituent ratio |
|---|---|---|
| Trophoblastic disease | 2 | 3.33% |
| Pregnancy abortion | 5 | 8.33% |
| Cervical pregnancy | 8 | 13.33% |
| CSP | 45 | 75.00% |

**Table 2.** Ultrasound detection and 3.0T MRI results

| Method | Diagnosis | Number |
|---|---|---|
| ultrasound | CSP | 37 |
| | misdiagnosis | 7 |
| | missed diagnosis | 8 |
| 3.0T MRI | CSP | 44 |
| | misdiagnosis | 1 |
| | missed diagnosis | 1 |

## Results

*Pathological diagnosis results*

The 60 patients were pathologically analyzed. Among these patients, 2 of whom were trophoblastic diseases, 5 were pregnancy abortion, 8 were cervical pregnancy, and 45 were CSP, as shown in **Table 1**.

*Comparison of pathological results with 3.0T MRI and ultrasound detection*

The results of ultrasound detection were 37 cases of CSP, 7 cases of misdiagnosis, and 8 cases of missed diagnosis; 3.0T MRI results were 44 cases of CSP, 1 case of misdiagnosis, and 1 case of missed diagnosis, as shown in **Table 2**.

*The diagnostic value of 3.0T MRI and ultrasound for CSP*

The sensitivity, specificity, coincidence rate, positive diagnosis rate, negative diagnosis rate, AUC, and 95% CI of 3.0T MRI in diagnosing CSP were significantly higher than those of ultrasound diagnosis ($P<0.05$), as shown in **Tables 3**, **4** and **Figure 1**.

## Discussion

The pathological feature of CSP after cesarean section is that after trophoblasts and fertilized egg is implanted, they would be surrounded by fibrous scar tissue myometrium. This is a type of ectopic pregnancy, and accounts for about 6.1% of all ectopic pregnancies [9-11]. The clinical symptom of CSP after cesarean section is vaginal bleeding during menopause, which is easily misdiagnosed as intrauterine pregnancy in clinical practice. If the patient is given drugs or surgical abortion, it can cause complications such as disseminated intravascular coagulation (DIC) and bleeding. If the patient continues pregnancy, complications such as abdominal pregnancy, placental implantation, and uterine rupture may occur, which risks patients' life. The main treatment methods for CSP include interventional therapy, drug therapy, hysteroscopic hysterectomy, and curettage [12]. Nowadays, many clinical researches preserve the fertility function of patients on the premise of ensuring the life and health of patients. It is reported that early diagnosis and treatment of CSP is beneficial for the quality of life of patients [13-15].

Menopausal history, medical history, imaging and laboratory test results should be considered when performing the clinical diagnosis of CSP. In general, the first step of screening is to implement ultrasound inspection, which can reveal the details of the cervix and uterus, and the relationship between the lower uterine segment and CSP [16]. Despite that the primary option for imaging is ultrasound, the study conducted by Zhang et al. [17] showed that ultrasound examination is not easy to distinguish CSP and trophoblastic tumors, both of which have a rich blood supply and are mostly low-speed and low-resistance types. Moreover, due to the low resolution of ultrasound detection, it is extremely easy to be infected by the patient's intestinal gas, bladder filling and other factors, further leading to misdiagnosis and missed diagnosis. 3.0T MRI has the advantages of high soft tissue resolution, multi-directional, multi-parameter and multi-sequence, and it is favorable for the evaluation of pelvic organ structure. Due to its property that can clearly determine the relationship between gestational sac, surgical scar and endometrial cavity, it has a high diagnostic value in the diagnosis of CSP. Therefore, 3.0T MRI clearly shows the relationship between the gestational sac and the cesarean section scar, which is essential for the correct diagnosis of CSP. It can also mea-

**Table 3.** The diagnostic value of 3.0T MRI and ultrasound for CSP

| Detection methods | sensitivity | specificity | coincidence rate | positive diagnosis rate | negative diagnosis rate |
|---|---|---|---|---|---|
| Ultrasound | 82.22% | 53.33% | 84.09% | 84.09% | 50% |
| 3.0T MRI | 97.78% | 93.33% | 96.67% | 97.78% | 93.33% |

**Table 4.** 3.0T MRI and ultrasound diagnosis of the area under the ROC curve

| Detection methods | AUC | P | 95% CI | |
|---|---|---|---|---|
| | | | Upper limit | Lower limit |
| Ultrasound | 0.681 | 0.00 | 0.051 | 0.776 |
| 3.0T MRI | 0.973 | 0.00 | 0.914 | 0.996 |

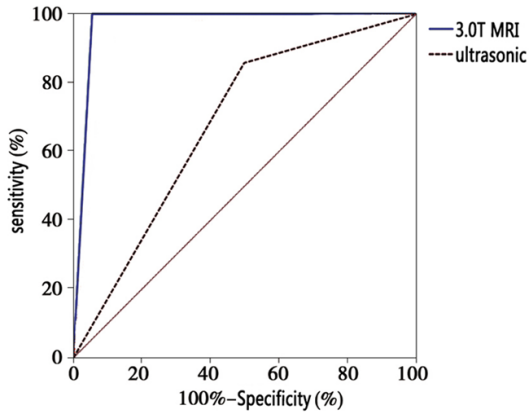


**Figure 1.** ROC curve of CSP detected by 3.0T MRI and ultrasound.

sure the volume of the lesion and observe whether the lesion and the uterus are bleeding, so it is helpful in the selection of conservative treatment and monitoring during treatment [17]. In addition, CSP is prone to placenta accreta, placental adhesions, placenta previa, etc., because 3.0T MRI shows a better placental edge. For placental conditions, including internal or external placental bleeding, fresh or old bleeding, early differential diagnosis can be made [18]. For cases that are difficult to diagnose by ultrasound, further examination should be performed and should all refer to the literature [17, 18]. Alexandra Stanislavsky [19] pointed out that 3.0T MRI can distinguish the relationship between the endometrium, cesarean section uterine scar, uterine cavity and gestational sac, and can clearly show the specificity of ectopic pregnancy.

We compared 3.0T MRI and ultrasound in diagnosing CSP after caesarean section, and found that the ultrasound detection showed 37 cases of CSP, 7 cases of misdiagnosis, and 8 cases of missed diagnosis; 3.0T MRI showed 44 cases of CSP, 1 case of misdiagnosis, and 1 case of missed diagnosis. This indicates that 3.0T MRI will not be affected by soft tissues and can clearly detect the blood flow signal, thereby reducing the rate of misdiagnosis and missed diagnosis. In our study, the sensitivity, specificity, coincidence rate, positive diagnosis rate, negative diagnosis rate, AUC and 95% CI of 3.0T MRI in the diagnosis of CSP were significantly higher than those of ultrasound diagnosis. This is similar to the conclusions of Rachel A [20] et al., indicating that 3.0T MRI in the diagnosis of CSP is better than ultrasound diagnosis.

To conclude, the coincidence rate of 3.0T MRI in the diagnosis of CSP after caesarean section is markedly better than that of ultrasound diagnosis. The limitation of the study includes that the sample size is small. The results of the study only provide an instruments reference for the clinical diagnosis of CSP after cesarean section. In the future, the sample size will be further increased, and multicenter research will be carried out.

## Acknowledgements

This work was supported by Medical Science Research Project of Hebei Province in 2019 (No. 20191761).

## Disclosure of conflict of interest

None.

**Address correspondence to:** Yajing Liu, Image Center, The People's Hospital of Hengshui City, No. 180, East Renmin Rd., Hengshui 053000, China. Tel: +86-0318-2181169; E-mail: yajingliu01@163.com

## References

[1] Wang J, Mujumdar AS, Deng LZ, Gao ZJ, Xiao HW and Raghavan GSV. High-humidity hot air

impingement blanching alters texture, cell-wall polysaccharides, water status and distribution of seedless grape. Carbohydr Polym 2018; 194: 9-17.
[2] Nagaraj UD, Calvo-Garcia MA and Kline-Fath BM. Abnormalities associated with the cavum septi pellucidi on fetal MRI: what radiologists need to know. AJR Am J Roentgenol 2018; 210: 989-997.
[3] Pilliod RA, Pettersson DR, Gibson T, Gievers L, Kim A, Sohaey R, Oh KY and Shaffer BL. Diagnostic accuracy and clinical outcomes associated with prenatal diagnosis of fetal absent cavum septi pellucidi. Prenat Diagn 2018; 38: 395-401.
[4] Liu D, Yang M and Wu Q. Application of ultrasonography in the diagnosis and treatment of cesarean scar pregnancy. Clin Chim Acta 2018; 486: 291-297.
[5] He J, Zhang J, Dai B and Liu P. Sequentially formations of Csp3-Csp2 and Csp2-Csp2 bonds by a one-pot reaction involving N-tosylhydrazone and p-bromobenzeneboronic acid. Chemistryselect 2019; 4: 4496-4498.
[6] Liu G, Xuan N, Rajashekar B, Arnaud P, Offmann B and Picimbon JF. Comprehensive history of CSP genes: evolution, phylogenetic distribution and functions. Genes 2020; 11: 413.
[7] Holz J, Pfeffer C, Zuo H, Beierlein D, Richter G, Klemm E and Peters R. In situ generated gold nanoparticles on active carbon as reusable highly efficient catalysts for a Csp3-Csp3 stille coupling. Angew Chem Int Ed Engl 2019; 58: 10330-10334.
[8] Huang Q, Zhang M and Zhai RY. The use of contrast-enhanced magnetic resonance imaging to diagnose cesarean scar pregnancies. Int J Gynaecol Obstet 2014; 127: 144-6.
[9] He J, Zhang J, Dai B and Liu P. Synthesis of 9-biarylfluorenes by one-pot, three-step reactions of N-tosylhydrazones, p-bromobenzeneboronic acid, and arylboronic acids. J Chem Res 2019; 48: 174751981985980.
[10] Pérez-Gómez M, Azizollahi H, Franzoni I, Larin EM, Lautens M and García-López JA. Tandem remote Csp3-H activation/Csp3-Csp3 cleavage in unstrained aliphatic chains assisted by palladium(II). Organomet 2019; 38: 973-980.
[11] Liu Z, Gao R, Lou J, He Y and Yu Z. Metal-free Csp-Csp and Csp-Csp3 bond cleavages of N, S-enynes toward thiophene-fused N-heterocycles. Adv Synth Catal 2018; 360.
[12] Nayak MK, Mukhi P, Mohanty A, Rana S, Arora R, Narjinari H and Roy S. Ni(II)/Al(0) mediated benzylic Csp3-Csp3 coupling in aqueous media. J Chem Sci 2019; 131.
[13] Paeth M, Tyndall S, Chen LY, Hong JC, Carson W, Liu X, Sun X, Liu J, Yang K, Hale E, Tierney D, Liu B, Cao Z, Cheng MJ, Goddard W and Liu W. Csp3-Csp3 bond-forming reductive elimination from well-defined copper(III) complexes. J Am Chem Soc 2019; 141: 3153-3159.
[14] Li C, Tong S, Wang K and Zhang X. Optimal CSP-1 boundary scheme based on the estimator of the proportion of conformance for specified in-control process. Cellular Logistics 2020; 17: 32-51.
[15] Mazzanti A, Drakopoulos A, Christina T and Kolocouris A. Rotation barriers of 1-adamantyl-Csp3 bonds measured with dynamic NMR. Chemistryselect 2019; 4: 7645-7648.
[16] Udhayasankar R and Karthikeyan B. Processing of cardanol resin with CSP using compression molding technique. Mater Manuf Process 2018; 34: 1-10.
[17] Zhang MW, Zhang GJ, Han ZG, Tian XM, Liu J, Gu SX, Wang SJ, Zhang D and Wang XZ. Diagnosis of caesarean scar pregnancy by magnetic resonance imaging. Obstet Gynecol Imaging 2012; 18: 436-438.
[18] Zhang X, Dai M, Yan ZH, Chen W and Chen Y. Magnetic resonance imaging diagnosis of caesarean section scar pregnancy of uterine. Genitourin Radiol 2011; 27: 1380-1382.
[19] Stanislavsky A and Goergen S. Echogenic cavum septi pellucidi is associated with mild callosal dysgenesis on postnatal MRI. Australas J Ultrasound Med 2019; 22.
[20] Pilliod RA, Pettersson DR, Gibson T, Gievers L, Kim A, Sohaey R, Oh KY and Shaffer BL. Diagnostic accuracy and clinical outcomes associated with prenatal diagnosis of fetal absent cavum septi pellucidi. Prenat Diagn 2018; 38: 395-401.